Tellus (2002), 54B, 850–871
Printed in UK. All rights reserved

TELLUS
ISSN 0280–6509

Transport of ^{222}Rn using the regional model REMO: a detailed comparison with measurements over Europe

By ANNE CHEVILLARD[1]*, PHILIPPE CIAIS[1], UTE KARSTENS[2], MARTIN HEIMANN[2], MARTINA SCHMIDT[3], INGEBORG LEVIN[3], DANIELA JACOB[4], RALF PODZUN[4], VICTOR KAZAN[1], HARTMUT SARTORIUS[5] and ERNEST WEINGARTNER[6], [1]*Laboratoire des Sciences du Climat et de l'Environnement, UMR CEA-CNRS 1572, F-91198 Gif-sur-Yvette, France;* [2]*Max-Planck-Institut für Biogeochemie, D-07701 Jena, Germany;* [3]*Institut für Umweltphysik, University of Heidelberg, Im Neuenheimer Feld 229, D-69120 Heidelberg, Germany;* [4]*Max-Planck-Institut für Meteorology, Hamburg, Germany;* [5]*Bundesamt für Strahlenschutz, Institut für atmosphärische Radioaktivität, Rosastrasse 9, D-79098 Freiburg, Germany;* [6]*Laboratory of Atmospheric Chemistry, Paul Scherrer Institut, CH-5232 Villigen, Switzerland*

(Manuscript received 9 July 2001; in final form 13 June 2002)

ABSTRACT

The ^{222}Rn concentration simulated by the regional atmospheric model REMO over Europe and western Siberia is compared to in-situ records in Europe, and discussed in the context of site effects for stations that are also part of a CO_2 observing network. The REMO model has a limited spatial domain, forced at its lateral boundaries with meteorological fields of the European Centre for Medium-Range Weather Forecasts and with tracer concentrations issued from the TM3 global transport model. The modelled ^{222}Rn field is compared to measurements at six stations: two coastal ones (Atlantic Ocean and Baltic Sea), two low-elevation sites in plains, one mountain station and one high-altitude station. We show that the synoptic and diurnal ^{222}Rn variability as simulated by REMO (55 km by 55 km) is realistic. In some cases REMO performs better than TM3, which is of coarser resolution, but this is not always true. At Mace Head, a station located near the western edge of the REMO domain, we show that the ^{222}Rn "baseline" concentration is strongly influenced by boundary conditions, reflecting ^{222}Rn transport from North America across the Atlantic Ocean. At Schauinsland, a mountain station in south-western Germany, even though the spatial resolution of REMO is not fine enough to reproduce transport processes induced by local topography, a fairly good agreement between model and measurements can be obtained, provided that one can determine from comparison of observed and modelled diurnal temperature changes which layer of the model is suitable for comparison with the data. Finally, the implications of modelling ^{222}Rn are discussed here in the broader context of interpreting site effects that may also affect CO_2 continental observations in Europe.

1. Introduction

Radon-222 (^{222}Rn) is a radioactive gas emitted by soils, and its concentration is sensitive to transport processes at synoptic scales. As such, ^{222}Rn is valuable to evaluate atmospheric transport in models as well as to study specific "site effects" at research stations where other atmospheric constituents are monitored. ^{222}Rn has been the object of previous studies to check the transport properties of global models (Liu et al., 1984; Jacob and Prather, 1990; Heimann et al., 1990; Ramonet et al., 1996; Jacob et al., 1997; Dentener et al., 1999), but little has been done using this tracer for regional models evaluation. In this paper, we test

*Corresponding author.
e-mail: anne.chevillard@irsn.fr
Present affiliation: Institut de Radioprotection et de Sûreté Nucléaire, DPRE/SERGD/LEIRPA, B.P. 17, F-92262 Fontenay-aux-Roses Cedex, France.

^{222}Rn simulated by the REMO regional model against a set of continuous measurements at six stations in Europe. The dataset includes marine and continental stations, as well as higher altitude stations over the period March 1998 until October 1998. We compared the modelled ^{222}Rn concentration with the observation on multiple time scales, ranging from diurnal to monthly.

This work addresses three main scientific issues, related to atmospheric transport processes over continental areas. Firstly, we wanted to check whether REMO was capable to reproduce the observed mean ^{222}Rn gradients (section 4), as well as the temporal variability (section 5) at the stations, a first step before applying the model to the transport of CO_2. Having an almost uniform source over continents and no source over the oceans, ^{222}Rn is naturally simpler to interpret than CO_2 which is associated to temporally and spatially variable fluxes. Secondly, we wanted to evaluate whether there is a gain in realism when using a high-resolution model such as REMO instead of a coarse resolution model such as TM3 (section 5). The REMO-TM3 comparison is legitimate, since both models use ECMWF meteorological fields to compute tracer advection, and have an identical convection scheme (Tiedtke, 1989). They differ, however, by their parameterisation of transport in the boundary layer and by the resolution of the advection. Given the higher complexity and computing demand of REMO, as well as its novelty in passive tracer transport applications, it was in fact important that such a new high resolution model could be compared to a widely utilized global model such as TM3. Thirdly, the comparison between our model results and observations shows that site-specific effects may bias the simulated ^{222}Rn concentration (section 6). We use various statistical criteria at each site to identify what are the sources of uncertainties associated with such "site effects" when reproducing at continental stations continuous observations. Two such site-specific sources of errors linked to the broader context of models are (1) the selection of an appropriate vertical level to match a mountain station, and (2) the selection of an appropriate grid box to match a coastal station. From a detailed study at typical mountain and coastal sites, we formulated practical solutions to obtain a more realistic simulation by improving the selection of the model output. Such selection criteria obtained from ^{222}Rn have broader implications as they can be applied for other species. In our case, at most of the stations where we studied ^{222}Rn, there exist co-located observations of CO_2. Hints on model transport and model selection that are derived from ^{222}Rn will thus have direct implications for the inverse modelling of regional sources and sinks of CO_2, a problem where the emissions are unknown but where model output selection issues are similar to those uncovered from ^{222}Rn.

2. Description of models

2.1. The REMO model

The regional model used in this study is REMO. The dynamical structure of the on-line REgional MOdel REMO is based on the regional weather forecast model "Europa-Model" (EM) of the German Weather Service (Majewski, 1991). REMO (version 4.3), with a DWD (Deutscher Wetterdienst) physical package, uses the hydrostatic approximation with 20 levels in a hybrid coordinate system, which implies layers of unequal thickness between the ground and 10 hPa. The model contains six vertical layers in the lower atmosphere up to 1 km at approximately 30, 130, 300, 500, 750, 1100 m. The horizontal resolution is 0.5° in a rotated spherical coordinate system whose equator is in the centre of the studied domain. The domain of the present study extends from western Europe to eastern Siberia (Fig. 1).

A description of the physical part of the model is given by Jacob and Potzun (1997), and a detailed study of the water budget is performed by Karstens et al. (1996) as a part of the BALTEX experiment. At lateral boundaries prognostic variables (such as air temperature, horizontal wind components and specific humidity) are forced every 6 h by the analysis data of the European Centre for Medium-Range Weather Forecasts (ECMWF). The time step of the physical part is 5 min. The period presented in this study extends from March 1998 to October 1998.

Langmann (2000) has developed in REMO the on-line transport of chemical tracers. Advective transport is solved explicitly according to the Smolarkiewicz (1983) scheme. Horizontal diffusive transport is neglected because numerical diffusion is already added to the system by the horizontal advection. Furthermore, the vertical diffusion coupled with vertical shears probably produces a stronger horizontal dispersion in the lower troposphere than the horizontal diffusion. Subgrid-scale vertical turbulent fluxes are calculated following the Louis (1979) scheme in the surface layer, and above the surface layer they are

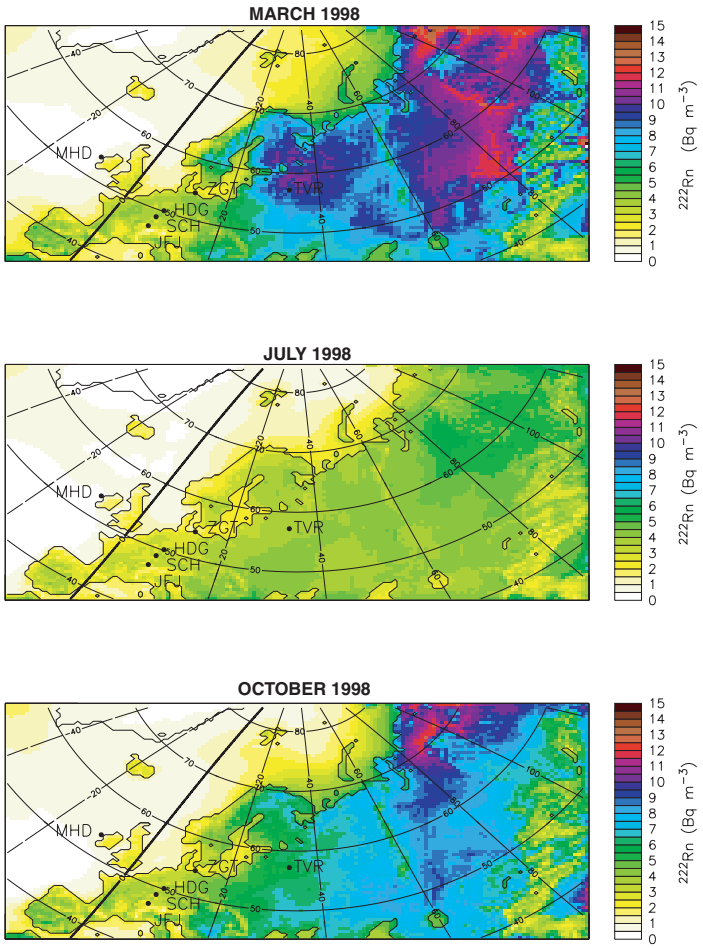

Fig. 1. March, July and October 1998 monthly average ^{222}Rn concentrations in the lowest model layer (about 30 m above ground). The stations discussed in the paper are Mace Head (MHD), Jungfraujoch (JFJ), Schauinsland (SCH), Heidelberg (HDG), Zingst (ZGT) and Fyodorovskoye (TVR).

deduced from a second-order closure scheme (Mellor and Yamada, 1974). Vertical transport of the tracer in convective clouds is identical to the transport of the liquid water in the physical part of the model (Tiedtke, 1989). The transport of the tracer has the same time step as the physical part (5 min), and for symmetry and stability reasons the sources and sinks of the tracer are considered every 10 min.

2.2. *The TM3 model*

A coarser resolution model, i.e. compared to REMO, is the global model TM3 (Heimann, 1995) that computes off-line the transport of tracers, based on ECMWF fields. Its horizontal resolution ($5^\circ \times 3.75^\circ$) is 75 times coarser than that of REMO. The TM3 model contains 19 vertical levels in sigma-coordinates, with four vertical layers below 1 km. Horizontal and vertical advection is calculated according to the Russel and Lerner scheme (1981). Convective transport is computed with the Tiedtke scheme (1989). Vertical diffusion is simulated according to the parameterisation of Louis (1979) in and above the surface layer. Comparison between REMO and TM3 is justified because both models use the same ECMWF fields (everywhere for TM3 and as boundary conditions for REMO) to compute transport, and have the same convection scheme.

3. Simulations of ^{222}Rn over Europe

Radon-222 is naturally formed in the radioactive decay chain of uranium-238, present in soils. Its major atmospheric sources are ice-free soils, whereas oceanic emissions are two to three orders of magnitude smaller (Wilkening and Clements, 1975; Lambert et al., 1982). The only significant sink of the chemically inert ^{222}Rn is its radioactive decay into polonium-218 (e-folding lifetime of 5.51 d). The configuration of the source–sink couple induces a strong vertical gradient of the atmospheric ^{222}Rn concentration, but also a clear difference between air masses of continental and oceanic origin, respectively. Therefore, ^{222}Rn is an excellent tracer to evaluate the performance of tracer transport parameterisation in atmospheric transport models.

Local measurements (Turekian et al., 1977) indicate large variations in ^{222}Rn exhalation rates from soils, from 0.1 to 2.5 atom cm^{-2} s^{-1}. Such variations depend mainly on soil texture (Dörr and Münnich, 1990), soil moisture (Nazaroff, 1992) as well as freezing or ice coverage (George, 1981). For example, high soil humidity and low water table depth decrease considerably the ^{222}Rn exhalation rate (Whittlestone et al., 1998; Levin et al., 2002), but data are lacking to describe these effects globally. Since no regional map of observed ^{222}Rn emissions covering the studied domain is available, we adopt a constant source of ^{222}Rn, of 1 atom cm^{-2} s^{-1} over continental areas and zero over oceans and regions with permanent ice coverage (Turekian et al., 1977).

Since the model domain does not cover the entire globe, a knowledge of the concentration of ^{222}Rn at the horizontal boundaries of the domain is required to solve the continuity equation. In the same way as meteorological fields computed by REMO are forced by external fields at the lateral boundaries, we prescribe in our standard simulation the ^{222}Rn concentration at REMO boundaries using the 3-hourly time varying ^{222}Rn concentration calculated from the global model TM3 (Heimann, 1995; Dentener et al., 1999). To ensure consistency in nesting REMO into TM3, the ^{222}Rn concentration is generated globally in TM3 with ECMWF transport fields that are identical for year 1998 to those used in REMO. Similarly, we prescribed to TM3 a ^{222}Rn source of 1 atom cm^{-2} s^{-1} over continental areas. We set the initial ^{222}Rn concentration in REMO equal to those produced by TM3, and further let it be transported by REMO. A test simulation was also performed using zero ^{222}Rn concentration for initial and boundary conditions. Comparison between the standard simulation and the test simulation is used to study the impact of long-range transport from outside into the REMO model domain.

4. European dataset of ^{222}Rn measurements

We compiled continuous ^{222}Rn measurements during the period March 1998 to October 1998 at six sites listed in Table 1. Two sites are coastal stations (Mace Head on the Atlantic Ocean and Zingst on the Baltic Sea), one site is at low elevation (Heidelberg) in the upper Rhine Valley (continental western Europe), one site is a mountain station in the Black Forest in Germany (Schauinsland) and one site is a high altitude alpine station in Switzerland (Jungfraujoch). One site operated as part of the EUROSIBERIAN CARBONFLUX project is the Russian station of Fyodorovskoye, for which we compared REMO output with data collected during July, August and October 1998, when intensive ground and aircraft measurements were carried out. All the data are presented in local winter time.

4.1. Fyodorovskoye, Russia

The Fyodorovskoye station (TVR) is located in European Russia, about 300 km north-west of Moscow

Table 1. *Characteristics of the stations*

Station	Location	Altitude (asl)	Period of observations	Characteristics
Mace Head	53°20′N, 9°54′W	5 m	96–99	Coastal station, Atlantic
Zingst	54°26′N, 12°44′E	1 m	98	Coastal station, Baltic Sea
Heidelberg	49°24′N, 8°42′E	116 m	98	Low elevation, western Europe
Fyodorovskoye	56°28′N, 32°55′E	265 m	98–99	Low elevation, eastern Europe
Schauinsland	47°55′N, 7°55′E	1205 m	98	Mountain, western Europe
Jungfraujoch	46°33′N, 7°59′E	3454 m	98	High altitude, western Europe

and 500 km south from the Baltic Sea. In July and August 1998, after the station was installed at 26 m above ground, the soil was almost saturated with water because of heavy rains that had occurred in early July 1998. The TVR data set is described by Levin et al. (2002). The measured ^{222}Rn activity during July–August 1998 is smaller by a factor of at least 2 than the one typically observed at continental sites in the same height above ground, with an average value of 1 ± 0.5 Bq m^{-3} over the whole period. The data exhibit a very small diurnal cycle, with a mean peak-to-peak amplitude of 1 Bq m^{-3} and higher values on average during the night-time. The soil type in the footprint of this site is sandy to loamy soil, with most areas in the landscape covered by an approximately 50 cm thick peat layer. The water table in the footprint of the tower lay between 5 and 70 cm in summer 1998. The measured ^{222}Rn exhalation rates were 10 times lower than those normally observed from this soil type when the water table is below several metres (Levin et al., 2002).

4.2. Mace Head, Ireland

The Mace Head station in Ireland (MHD) is located 5 m above sea level (asl). The hourly activity of ^{222}Rn daughters has been monitored since June 1995 (Biraud et al., 2000). At MHD, the meteorological situation is mainly influenced by the westerly passage of frontal systems, originating from the north Atlantic Ocean, but also, occasionally, by easterly winds delivering air with elevated concentrations of ^{222}Rn and anthropogenic compounds from Europe (Bousquet et al., 1996). MHD is a marine background station that is also reached by continental air, either from local origin (Ireland) or from a more remote origin (north-western Europe). The ^{222}Rn baseline defined from air masses classified in the marine sector (Biraud et al., 2000) is less than 0.3 Bq m^{-3}, whereas ^{222}Rn "events" from Europe can reach up to 5 Bq m^{-3}. In summer time, diurnal variations in ^{222}Rn are also frequently observed, associated with sea-breeze effects and influenced by emissions from Irish soils, with maxima during the night and minima at around noon.

4.3. Heidelberg, Germany

At Heidelberg (HDG) an ^{222}Rn monitor has provided half-hourly measurements of ^{222}Rn daughters since 1995 (Levin et al., 2002). It is installed on the roof of the Institut für Umweltphysik building, about 20 m above the ground. Radon-222 activities range from 1 to 30 Bq m^{-3} in August. Contrary to the measurements at TVR and MHD stations, ^{222}Rn at HDG presents a clear diurnal cycle with a maximum around sunrise and minimum values in the early afternoon, when the atmospheric boundary layer (ABL) is most developed.

4.4. Zingst, Germany

The station of Zingst (ZGT) is situated 300 m south of a sand beach on a peninsula, facing the Baltic Sea. The station is between forests (east side) and meadows (west and south side). At about 2 km south of the station, the soil is usually waterlogged (salted and fresh). Measured activities of ^{222}Rn are usually smaller than at HDG, with an average value of 2 Bq m^{-3} and maxima of up to 8 Bq m^{-3} (Schmidt, 1999). The data exhibit a diurnal cycle of small amplitude, with an ^{222}Rn maximum in the morning, before the air of the stable nocturnal boundary layer is vertically diluted. However, the amplitude of the diurnal cycle at ZGT is 3–5 times lower than at HDG, probably due to lower ^{222}Rn emissions by soils near ZGT (Cuntz, 1997) and to the proximity of the Baltic Sea.

4.5. Schauinsland, Germany

Schauinsland (SCH) is located 10 km south of Freiburg in the Black Forest, 1205 m asl, on a mountain ridge above the Rhine Valley. It is operated by the Bundesamt für Strahlenschutz, Freiburg, Germany. SCH is considered as a continental regional background station (Levin et al., 1995). Radon-222 measurements range from 1 to 10 Bq m^{-3} and show large differences between night-time and daytime. During night-time, SCH is usually above the boundary layer, while at daytime, particularly in summer, the station most frequently lies in the convective boundary layer (Schmidt et al., 1996). Generally, air masses measured at SCH during the night are relatively well mixed and are influenced by sources from several hundred kilometres away. In contrast, during the day, SCH is reached by air rising up from the surrounding valleys and is most likely of more local origin. In summer, maximum ^{222}Rn concentrations are observed at around 12:00 pm and in winter at around 14:00 pm, driven by the diurnal variations of the depth of the atmospheric boundary layer.

4.6. *Jungfraujoch, Switzerland*

The Jungfraujoch station (JFJ) is the highest research station in Europe (3454 m asl) and part of the GAW program as a continental background site. Radon-222 data were measured by means of an epiphaniometer (Gäggeler et al., 1995). In winter ^{222}Rn concentrations are usually smaller than 1 Bq m^{-3} with no diurnal cycle. In spring (April–May–June) maximum ^{222}Rn concentrations of up to 6 Bq m^{-3} in the late afternoon are observed, with diurnal variations superimposed on synoptic events lasting several days. In summer (July–August–September) diurnal cycles predominate, although of smaller amplitude on average than during spring, with maxima in the late afternoon. Diurnal changes in vertical mixing rather than in horizontal advection have been suggested to be the main source of the observed summer diurnal ^{222}Rn variability (Lugauer et al., 2000). During summer, the station is often influenced in the early afternoon by air from the planetary boundary layer through thermally driven transport, while at other times and seasons the station is rather uncoupled from the boundary layer, and therefore not contaminated by nearby emissions (Lugauer et al., 1998).

5. Mean spatial and seasonal patterns

5.1. *Horizontal gradients*

Figure 1 shows the monthly average simulated ^{222}Rn field in the lowest model layer (at about 30 m asl) during March, July and October 1998. There is a seasonal cycle in the continental mean ^{222}Rn concentration, with lower values in July (3.9 Bq m^{-3} over land) than in March and October (7.3 and 6.2 Bq m^{-3}, respectively). The seasonality results from enhanced vertical motion in summer when ^{222}Rn emitted from soils is distributed into a higher convective boundary layer. Dentener et al. (1999) were able to reproduced similar broad-scale patterns with much coarser transport models.

Higher average ^{222}Rn values are predicted by REMO (Fig. 1) over the interior of Eurasia, ranging from 1.5 to 20 Bq m^{-3}, in contrast with lower ^{222}Rn values over the oceans of less than 1.0 Bq m^{-3}. In our test simulation (not shown) without ^{222}Rn boundary conditions, the predicted ^{222}Rn concentration would rapidly drop to zero from the continents towards the Atlantic Ocean within a distance of 1000 km from the coast. In the standard simulation, however, we predict a significantly higher ^{222}Rn baseline over the North Atlantic, close to 0.6 Bq m^{-3} on average (Fig. 1), which is attributed to the intrusion of continental air masses from regions external to the REMO domain (e.g. North America). On average in all months, there is nevertheless a continentality gradient in the surface ^{222}Rn concentration with an increase from west to east (Fig. 1). This continentality gradient becomes more pronounced during March and October than in July (Fig. 1). Over mountains, the modelled ^{222}Rn concentration is smaller than in surrounding plains. In elevated model grid cells, the local ^{222}Rn soil source is identical (1 atom cm^{-2} s^{-1}) to the one of lower level grid cells, but ^{222}Rn emitted locally is mixed up with tropospheric air that has already been depleted in ^{222}Rn by dilution and radioactive decay.

5.2. *Vertical gradients*

We divided arbitrarily the REMO domain into three distinct regions in longitude: a western (40°W to 20°E), a central (20°E to 60°E) and an eastern (60°E to 120°E) region. Figure 2 (right side) shows the simulated ^{222}Rn vertical profiles in these three regions. Overall, there is a marked decrease in the mean ^{222}Rn activity with altitude, linked to vertical transport and radioactive decay, that is qualitatively consistent with atmospheric measurements compiled by Liu et al. (1984) (Fig. 2, left side). Profiles from Liu et al. measured between 9:00 and 13:00 are then compared with modelled profiles in REMO between 10:00 and 17:00. The daytime selected model outputs differ from the unselected profiles only below 1.5 km and in summer, when diurnal variations of the mixed layer are large. The shape of the simulated vertical profiles varies throughout the year, with stiffer and more homogeneous profiles in summer over all three west, central and east regions (Fig. 2). In July, as opposed to October, stronger vertical mixing generates a deficit of ^{222}Rn below 1 km, and conversely an excess aloft. Figure 2 also shows that the continentality gradient in longitude simulated at the ground level (Fig. 1) is persistent over the entire air column up to about 5 km.

6. Comparison between REMO, TM3 and observed ^{222}Rn records

We compare the REMO model output with observations that exhibit variability going from diurnal cycles to synoptic changes and seasonal variations. The

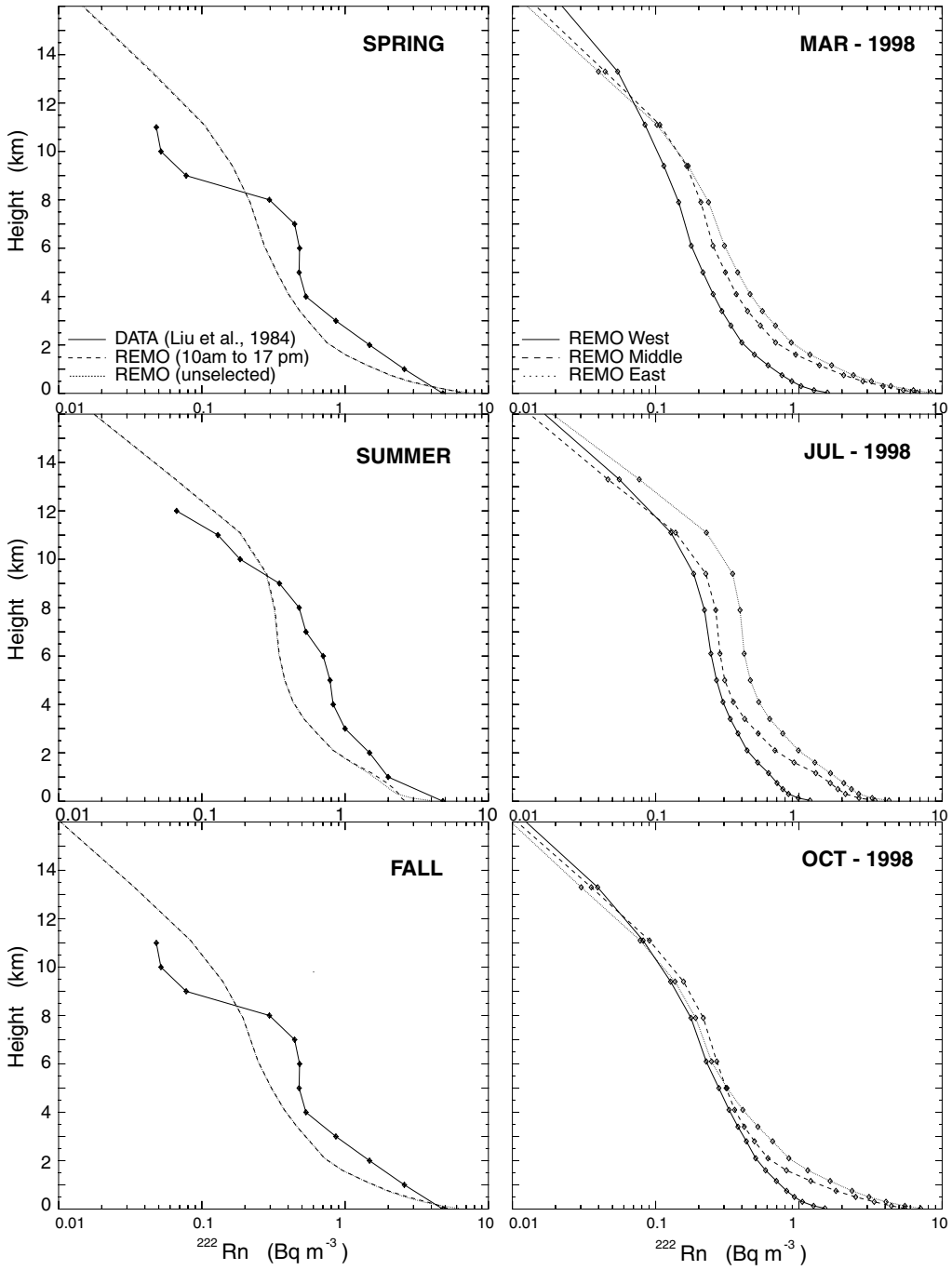

Fig. 2. Variations of the vertical profile of ^{222}Rn monthly mean concentration. Left side: The average over land simulated with REMO (dotted line) is compared with Liu et al. (1984) (solid line) in spring, summer and autumn Right side: The simulated longitudinal gradient is presented for March, July and October for three regions: west (solid line, 40°W to 20°E), middle (dashed line, 20°E to 60°E) and east (dotted line, 60°E to 120°E).

Table 2. *Monthly mean ^{222}Rn concentration (Bq m^{-3}) observed and simulated by REMO and TM3*[a]

	March 1998			July 1998			October 1998		
	Obs.	REMO	TM3	Obs.	REMO	TM3	Obs.	REMO	TM3
MHD	0.4	**0.5**	0.6						
	(±0.3)	(±0.3)	(±0.1)						
ZGT	1.2	3.7	**2.4**	1.2	2.7	**2.6**	1.6	3.8	**2.4**
	(±0.5)	(±1.0)	(±0.7)	(±0.6)	(±0.9)	(±0.6)	(±0.9)	(±1.2)	(±0.7)
HDG	3.4	**3.8**	4.2	4.3	3.3	**3.7**	4.7	3.6	**3.9**
	(±1.1)	(±1.0)	(±1.2)	(±1.2)	(±0.9)	(±1.0)	(±1.4)	(±0.9)	(±1.0)
SCH – A	1.5	2.6	4.5	2.6	**2.7**	3.7	2.0	2.8	4.1
	(±0.6)	(±0.6)	(±1.2)	(±0.5)	(±0.6)	(±1.0)	(±0.7)	(±0.5)	(±1.1)
SCH – B		**1.1**	2.0		1.2	1.7		1.3	**2.5**
		(±0.2)	(±0.3)		(±0.2)	(±0.2)		(±0.3)	(±0.7)
JFJ – A	0.4	1.5	4.1	0.7	1.6	3.7	0.3	1.8	3.7
	(±0.3)	(±0.3)	(±1.0)	(±0.3)	(±0.4)	(±0.9)	(±0.2)	(±0.4)	(±0.9)
JFJ – B		**0.5**	1.4		**0.8**	1.3		**0.7**	1.6
		(±0.1)	(±0.3)		(±0.2)	(±0.2)		(±0.2)	(±0.5)
TVR				1.3	**3.7**	5.7	1.6	5.5	**4.8**
				(±0.3)	(±0.8)	(±1.0)	(±0.7)	(±1.4)	(±0.7)

[a]At Schauinsland, two levels are documented: SCH-A corresponds to the surface layer of each model (ca. 30 m above model ground) and SCH-B to the layer of each model at the true altitude of the station (1205 m). The same holds at Jungfraujoch, where JFJ-B is 2850 m. Bold numbers indicate which model best matches the measurements.

model–data comparison is based on statistical analysis, monthly averages (Table 2), absolute and relative amplitudes of the monthly mean diurnal cycle (Tables 3 and 4) and figures of merit (Table 5). Firstly we present the REMO and TM3 comparison with observations at each station in March, July and October 1998. Secondly, we study at each site the variability occurring at specific diurnal and seasonal time scales.

6.1. Comparison at each station

Figure 3 compares the modelled and observed hourly ^{222}Rn concentration in March 1998 at **Mace Head**. At this marine station, the measurements (solid line) show a low baseline (<0.5 Bq m^{-3}) with no diurnal cycle, and large peaks (>2.5 Bq m^{-3}). Peaks in ^{222}Rn are mainly related to shifts from marine to continental air (Biraud et al., 2000) as evidenced by changes in wind direction (Fig. 3). When the winds come from the south to north–west (180 to 315°), the ^{222}Rn concentration is close to the baseline. On the contrary, when the winds come from the east, ^{222}Rn concentrations are higher than 1 Bq m^{-3}, and the station is exposed to air masses influenced by Irish or European sources. Easterly wind speeds are usually smaller than westerly ones (Fig. 3), which increases the

Table 3. *Amplitude (Bq m^{-3}) of the monthly mean diurnal cycle of ^{222}Rn concentration with same conventions as in Table 2*

	March 1998			July 1998			October 1998		
	Obs.	REMO	TM3	Obs.	REMO	TM3	Obs.	REMO	TM3
MHD	4.1	**2.7**	2.1						
ZGT	4.9	10.0	**6.9**	8.0	**10.0**	5.3	13.7	**13.6**	5.4
HDG	16.5	9.9	**11.8**	14.9	8.4	**10.8**	13.0	7.6	**12.0**
SCH – A	6.8	**4.7**	13.0	6.2	**5.4**	11.5	6.7	4.2	13.9
SCH – B		2.1	3.2		2.6	2.6		3.2	**4.7**
JFJ – A	5.7	**3.4**	9.2	2.9	**3.5**	10.6	1.6	4.9	12.1
JFJ – B		1.7	2.5		1.9	1.9		**2.0**	3.4
TVR				3.6	**7.3**	9.5	7.5	12.0	**8.2**

Table 4. *Relative amplitude of the monthly mean diurnal cycle of ^{222}Rn concentration*[a]

	March 1998			July 1998			October 1998		
	Obs.	REMO	TM3	Obs.	REMO	TM3	Obs.	REMO	TM3
MHD	9.1	**5.3**	3.7						
ZGT	4.0	2.7	**2.8**	6.8	**3.7**	2.0	8.2	**3.5**	2.2
HDG	4.8	2.6	**2.8**	3.4	2.6	**3.3**	2.7	2.2	**2.9**
SCH – A	4.4	1.8	**2.9**	2.4	2.0	3.1	3.3	1.7	**3.4**
SCH – B		2.0	1.6		**2.1**	1.5		2.5	1.9
JFJ – A	13.9	2.3	2.3	4.2	2.1	**2.8**	5.2	2.7	**3.2**
JFJ – B		3.6	1.8		2.3	1.5		2.8	2.1
TVR				2.8	**2.0**	1.7	4.6	**2.2**	1.8

[a]The relative amplitude is defined as the amplitude of the average monthly diurnal cycle relative to the monthly average concentration.

exposure of air reaching MHD to local ^{222}Rn sources. The REMO model matches well the timing, the duration and the amplitude of most measured ^{222}Rn peaks (Fig. 3). The model, however, simulates a small peak on March 8–9, which is not in the observations, and conversely does not capture the occurrence of high ^{222}Rn values on March 18–19. In both cases the discrepancy between model and data occurs when the wind speed is very low, and when very local conditions may prevail (Fig. 3). At MHD, possibly because of its coarser resolution, TM3 is generally worse than REMO and fails to capture the sharpness of changes in ^{222}Rn concentration associated to shifts in wind direction. Nevertheless, REMO and TM3 do reproduce correctly the monthly mean values in March (Table 2).

Table 5. *Monthly mean figures of merit of modelled ^{222}Rn concentration compared to the observations*[a]

	March 1998		July 1998		October 1998	
	REMO	TM3	REMO	TM3	REMO	TM3
MHD	**0.56**	0.47				
ZGT	0.34	**0.50**	**0.42**	0.39	0.41	**0.50**
HDG	0.66	**0.67**	0.68	**0.73**	0.69	0.69
SCH – A	0.49	0.37	**0.68**	0.65	0.63	0.50
SCH – B	**0.65**	0.62	0.51	0.67	0.63	**0.69**
JFJ – A	0.23	0.1	0.37	0.20	0.17	0.08
JFJ – B	**0.47**	0.22	**0.52**	0.43	**0.34**	0.17
TVR			**0.38**	0.26	0.32	**0.34**

[a]The figure of merit is defined as the ratio of the two areas: min(measurements, model) and max(measurements, model). This quantity is close to 1 when both modelled and observed time series have similar phase and amplitude.

Boundary conditions of ^{222}Rn, as prescribed here from TM3, do exert an influence on REMO results at MHD. The test simulation with zero ^{222}Rn at the boundaries produced an almost zero ^{222}Rn activity under westerly winds, which is unrealistic, whereas including boundary conditions brings up the marine baseline close to the observed one (see Fig. 12 later).

Figure 4 compares simulation and observation at **Zingst**. The ^{222}Rn data exhibit (1) intervals of low baseline concentrations, although slightly higher than at MHD with no obvious diurnal cycle, (2) intervals with diurnal variability lower than 3 Bq m^{-3}, where minimum values are close to the baseline (e.g. 10–12 and 15–16 March), and (3) synoptic events with elevated ^{222}Rn concentrations reaching up to 4 Bq m^{-3}. Such distinct variability regimes are correctly reproduced by REMO, except that the minimum baseline ^{222}Rn values are always overestimated in the model (2 Bq m^{-3} instead of 0.5 Bq m^{-3}), which may be caused by an overestimate of regional ^{222}Rn emissions from soils (Cuntz 1997; Schmidt 1999). The measured ^{222}Rn concentration is always lower than 1.5 Bq m^{-3} when the wind is coming from the sea (west to northeast), and it is higher than 2.0 Bq m^{-3} when the wind comes from the continent (south). In REMO as well, lower (higher) ^{222}Rn concentrations indeed prevail when the wind comes from the sea (land). The ^{222}Rn values are largely overestimated in the land sector (Fig. 4). The location of ZGT, on a peninsula, is certainly the main reason for this deficiency of REMO. Criteria for a "best" possible selection of the model grid box better to compare with observations are given in the discussion (section 6). REMO overestimates both the mean ^{222}Rn value and the diurnal cycle

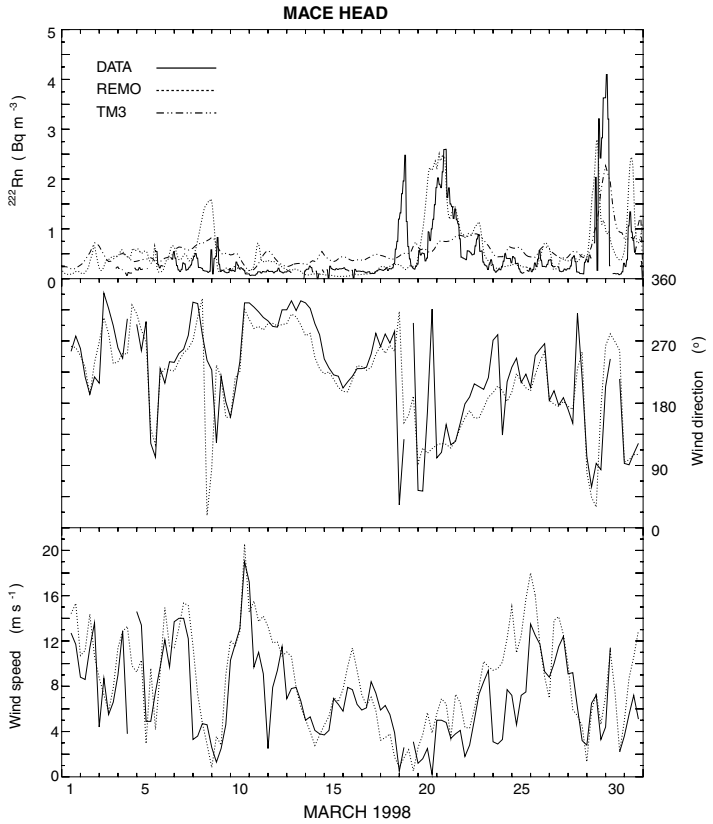

Fig. 3. Upper panel: observed and simulated ^{222}Rn concentration at Mace Head. Middle panel: wind direction (90 = east). Lower panel: wind speed. Solid line, observation; dotted line, REMO; dash-dot-dot line, TM3.

amplitude (Tables 2 and 3), a larger mean concentration resulting from larger surface emissions and inducing a larger diurnal cycle (discussion in section 7). Moreover, the wind direction modelled by REMO is often unrealistic (Fig. 4), indicating a bad representation of the local meteorology at this station. In contrast, TM3 is forced everywhere by the ECMWF analysis, which is closer to the wind observations. As a consequence, at ZGT the TM3 model generally better matches the data than REMO (Fig. 4). At this station a better representation of the meteorology is more important than an increase of the spatial resolution.

At **Heidelberg** the simulated ^{222}Rn in REMO matches the observations very well for all three months. At this station, where pronounced diurnal variations are apparent, the daily minima in ^{222}Rn concentration reflect the content of the well mixed ABL. Low minima suggest that the ABL growth entrains air from aloft which is poor in ^{222}Rn, as it has been separated from the surface for several days. High minima during several consecutive days generally reflect stable conditions with low wind speed and long continental residence times of tracers. In March (Fig. 5), both modelled and observed minima agree fairly well, with low values of 2 Bq m^{-3} (13–25 March) followed by higher minima of 3 Bq m^{-3} (26–29 March). In July, the climate simulated by REMO frequently differs from the observed fields inside the domain. Nevertheless, we count 21 days (Fig. 6) for which the minima of modelled and observed ^{222}Rn concentration differ by less than 0.5 Bq m^{-3}, which is quite good. In October (Fig. 7), the modelled and observed ^{222}Rn disagree between 1–10 October and agree with each other after 20 October, with a sharp decrease of ^{222}Rn by 23 October when diurnal cycles disappear. Overall, if the ^{222}Rn minima are well reproduced by REMO, the maxima, especially in July, are underestimated. Maxima are observed at the end of the night when the

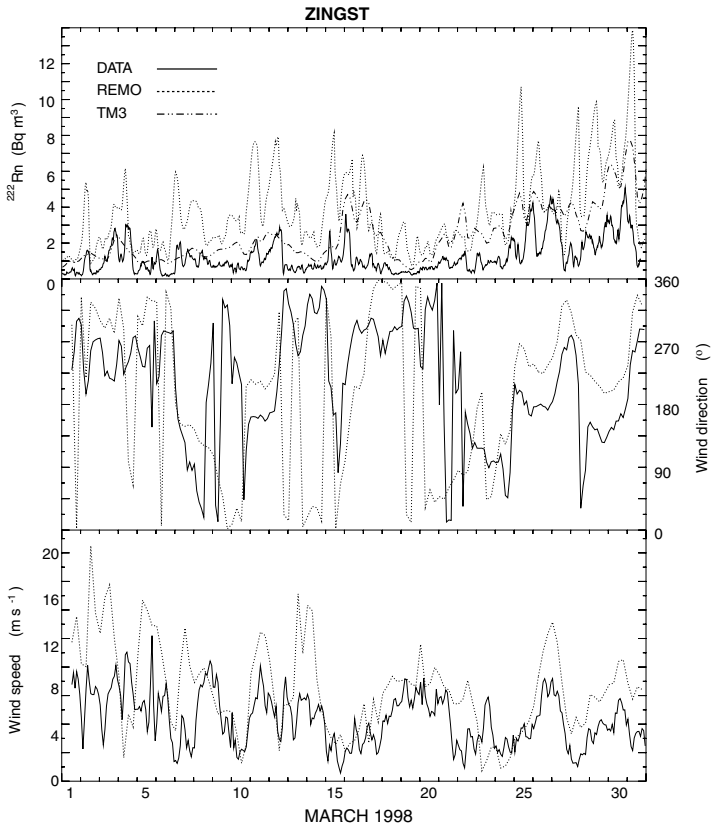

Fig. 4. Same as Fig. 3, but for Zingst on the Baltic Sea.

nocturnal boundary layer is stratified. The top of the lowest REMO layer is 60 m high, whereas measurements are made 20 m above ground. The accumulation of ^{222}Rn is observed to take place near the ground in the nocturnal boundary layer, yielding a steep vertical gradient which is not resolved in REMO. When comparing REMO with TM3 (Tables 2–5), both models produce a good agreement with the data, with a slight advantage to TM3, probably due to a better representation of the meteorology used by TM3 (ECMWF analysis)

At **Schauinsland** (altitude 1205 m) peaks of ^{222}Rn concentration are observed (Levin et al., 1995; Schmidt et al., 1996) when radiative warming of the surface promotes convection and transports ^{222}Rn-rich air from the nearby Rhine Valley to the station. SCH thus belongs either to the ABL during day and summer time or to the free troposphere during winter time (and during summer time at night). Comparing model results with measurements thereby proves relatively difficult, since the model does not resolve the mountain topography. The ground altitude of the REMO grid cell containing SCH is 730 m (layer 1). Comparison with data can be performed either for this layer or for the real altitude of the station (layer 4), as shown in Figs. 5–7. The time series of ^{222}Rn observations can be separated into distinct regimes: (1) small daily mean and small daily amplitude (0.5–2.0 Bq m^{-3}) with a weak maximum in the early afternoon, (2) high daily mean and large amplitude (1–6 Bq m^{-3}) with a sharp maximum in the early afternoon and (3) high daily mean and large amplitude but with maximum concentration occurring in the morning following accumulation in night-time. The first regime is typical of free troposphere variations of tracers emitted at the surface and occurs mainly in winter (e.g. 13–22 March, 12–15 and 24–30 October). The second regime (e.g. 27–31 March) corresponds to synoptic situations yielding high daytime values in plains surrounding SCH, as confirmed by the HDG (Fig. 5) and Freiburg data nearby (not

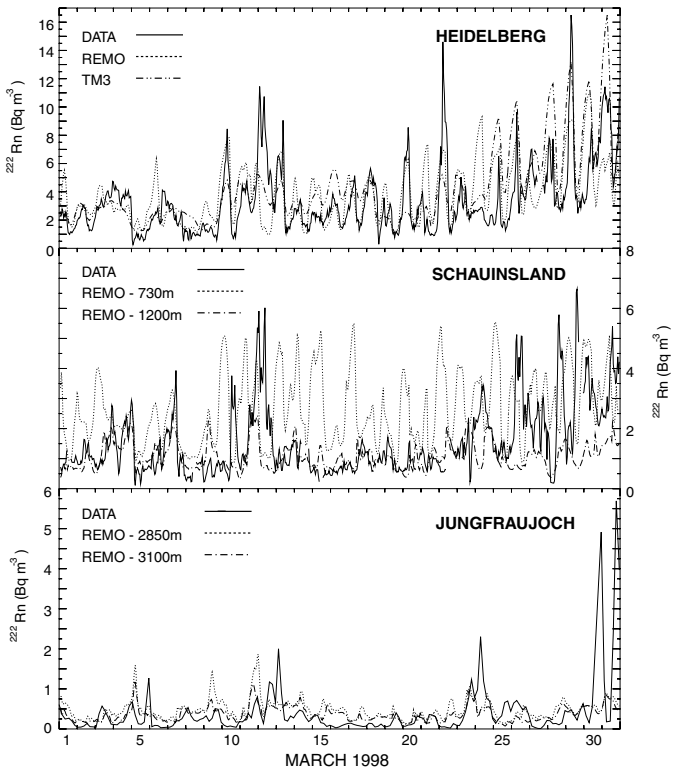

Fig. 5. ^{222}Rn concentration during March 1998 at Heidelberg (upper panel), Schauinsland (middle panel) and Jungfraujoch (lower panel). Measurements are given by the solid line. REMO results are shown at different heights above sea level. At Schauinsland (respectively Jungfraujoch) the dotted line represents the concentration at 730 m (2850 m) and the dash-dot line shows the concentration at 1200 m (3100 m). TM3 results are presented by the dash-dot-dot line at Heidelberg only.

shown). Weather maps further suggest that this regime reflects a stable high-pressure situation, with low wind speeds, during which a large-scale regional accumulation of ^{222}Rn develops. The third regime occurs frequently in summer, when SCH lies within the ABL.

Under the first regime, frequent in winter, REMO best reproduces the data when sampled at the real altitude of the station (layer 4). Under the third regime, the best match is obtained at the surface (layer 1). We tried to evaluate further the vertical mixing in REMO using the observed vertical gradient in ^{222}Rn observations between Freiburg (200 m) and SCH (1205 m). Both stations are in the same REMO grid box, so we had to pick up the closest low-elevation grid box to simulate Freiburg. Under the first regime, we verified that the vertical gradient between Freiburg and SCH is well reproduced, suggesting realistic mixing rates among the lowest layers of REMO (Fig. 8).

Comparing REMO and TM3 to observations in Tables 2 and 5 for monthly averages and figures of merit indicates that REMO reproduces the data better than TM3, when the station is placed in layer 1 in July and in layer 4 in March. Results in Tables 2 and 5 illustrate, more generally, that when attention is paid to place a mountain station in the appropriate model layer, a significant improvement of the model–data comparison can be obtained.

At **Jungfraujoch** station (Figs. 5–7) low ^{222}Rn values alternate with peaks. The model reproduces rather well the mean ^{222}Rn value and the mean variability, indicating that the vertical attenuation of ^{222}Rn with height is properly captured with the model parameterisation of vertical mixing processes (Fig. 2). As for SCH, we compare the ^{222}Rn data with the model layer 5 (2850 m) located at 750 m above the REMO local topography. The REMO results are in that case within the range of the observations. On the other hand, ^{222}Rn

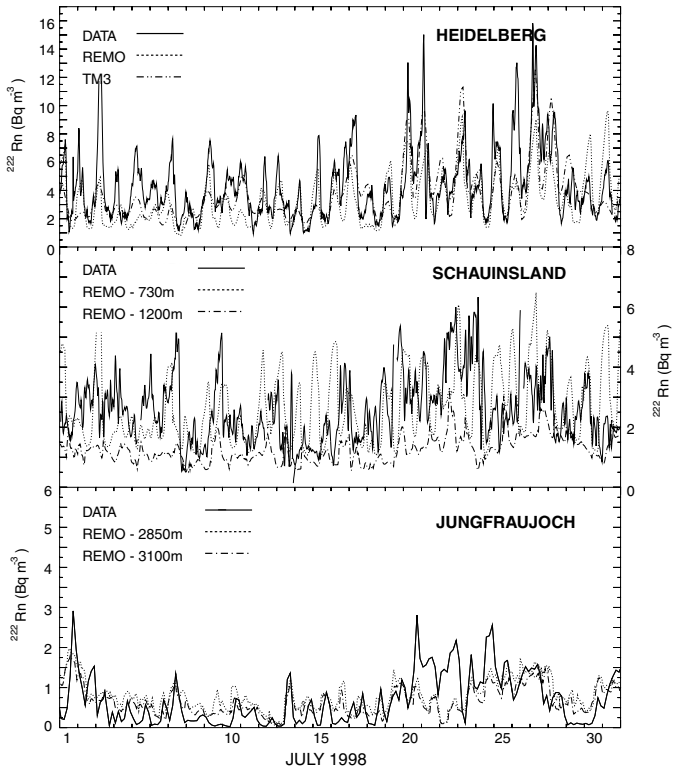

Fig. 6. Same as Fig. 5, but for July 1998.

in the layer 1 would be unrealistically high (Table 2), indicating that the station is not directly influenced by the planetary boundary layer (Nyeki el al., 1998). Statistics in Tables 2 and 5 further confirm that the concentration simulated in layer 5 (JFJ-B) is closer to the observations than the surface layer. In July, REMO produces higher average ^{222}Rn concentrations compared to March and October and reproduces the observations well. The diurnal cycle amplitude in July is also slightly higher than in March and October. In October, however (21–30 October) the model is not capable of reproducing the very low baseline concentrations even though the meteorology in REMO is correct (Fig. 7). This may reflect too strong vertical mixing intensity (see also Fig. 2). It also suggests that REMO is slightly more realistic at JFJ than TM3.

The **Fyodorovskoye** site is very atypical. One would expect the ^{222}Rn mean value at this very continental station to be higher than in HDG (Fig. 1), and to exhibit large diurnal cycles as well. This is, however, not the case. Observed ^{222}Rn concentrations were low during July–August 1998 (Fig. 9), i.e. three times lower than in HDG with an equally smaller diurnal cycle amplitude (Tables 2 and 3). The most likely explanation lies in considerably reduced ^{222}Rn emissions from soils in the TVR area, due to generally very wet or even water-saturated soils. As mentioned previously, ^{222}Rn exhalation in the immediate surroundings of the TVR site was about a factor of 10 lower than, e.g., around HDG (Levin et al., 2002). In addition, the modeled meteorology at TVR is correctly reproduced in REMO, which shows that the ^{222}Rn source variability may be critical in such cases for determining the atmospheric concentration. The figure of merit results (Table 5) outline the failure at this site of both REMO and TM3 to reproduce the measurements.

6.2. Average diurnal cycles

Overall, the amplitude of the diurnal cycle is positively correlated with the daily mean ^{222}Rn concentration, as expected from the modulation of near-surface ^{222}Rn by the daily oscillation of the boundary layer depth. This is the reason why we prefer to present in

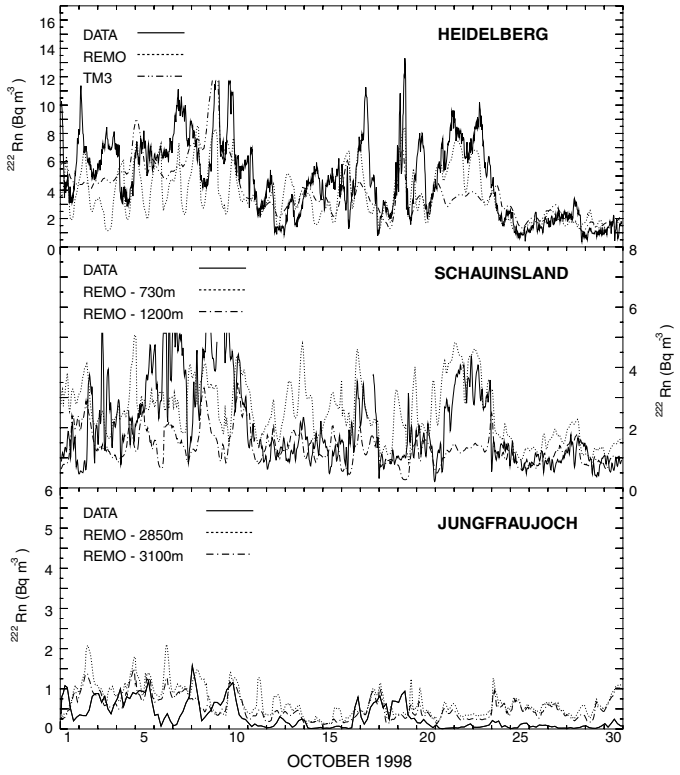

Fig. 7. Same as Fig. 5, but for October 1998.

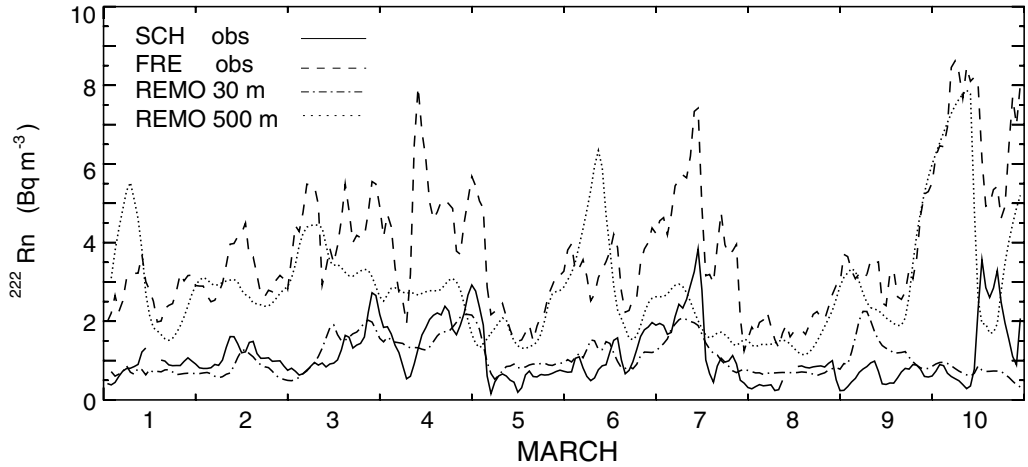

Fig. 8. ^{222}Rn concentration during March 1998 (first regime) observed at Schauinsland (solid) and Freiburg (dash), and simulated in the closest low-elevation grid box (dash-dot) and simulated at Schauinsland at 500 m (dot).

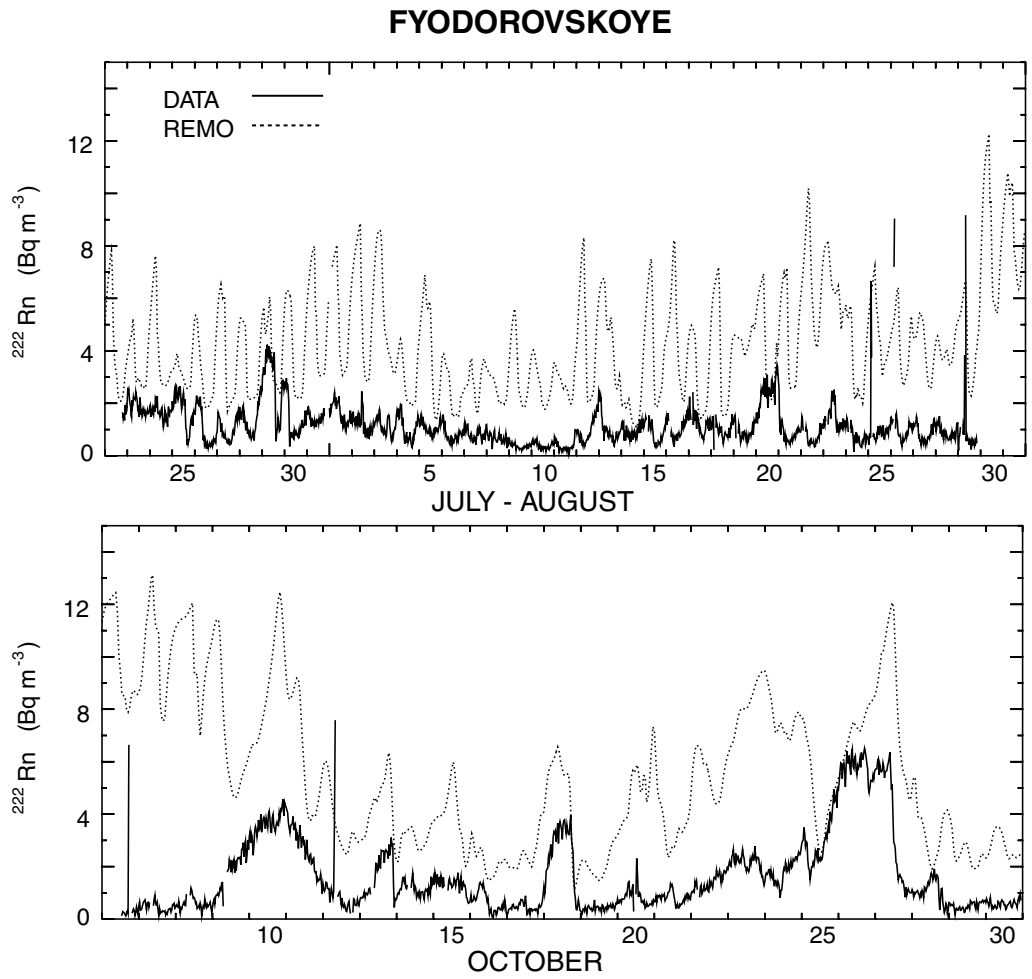

Fig. 9. ^{222}Rn concentration during July, August and October 1998 at Fyodorovskoye. Measurements are represented by the solid line and REMO results by the dotted line.

Fig. 10 and Table 4 the relative amplitude (RA), obtained by dividing the amplitude by the mean concentration both in the data and in the model, a more robust quantity for model–data comparison. At **Mace Head** in winter, there is no diurnal cycle, which is well captured in both models. At **Zingst**, the modelled RA is overestimated in REMO in winter, whereas it is underestimated in TM3 in summer. In May both models do not capture well the phase of the RA at ZGT, probably because of incorrect representation of the boundary layer diurnal oscillation. At **Heidelberg** both REMO and TM3 reproduce rather well the observed RA, with REMO doing better in May and in July. At **Fyodorovskoye** the modelled RA is captured correctly, with REMO showing a better phase agreement than TM3. Interestingly, both models grossly overestimated the mean concentration, and thus the absolute diurnal amplitude (Fig. 9), at this site, but using RA cancels out the impact of the source magnitude when applied to both data and models. At **Schauinsland**, when the site is sampled in the appropriate model layer (section 5.1) both REMO and TM3 are very good at reproducing the RA, except in July: then the models overestimate the RA, as they are not able to reproduce subgrid-scale transport processes which mix the air over the Rhine Valley to deliver it by noon at the

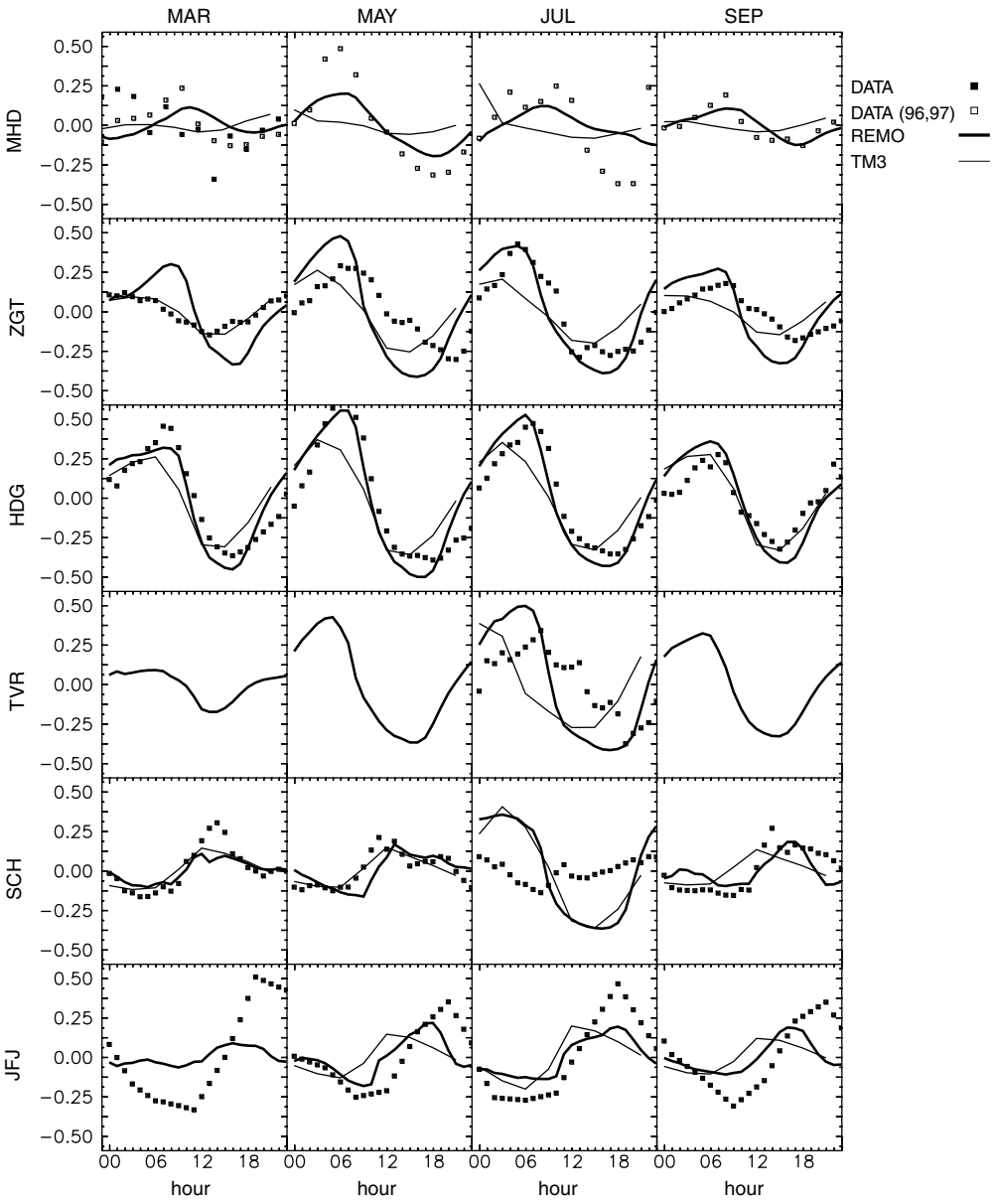

Fig. 10. Monthly average diurnal cycle of ^{222}Rn concentrations (relative amplitude) calculated for March, May, July and September 1998 at six stations in Europe. Measurements are represented by filled squares; open squares show the average diurnal cycle of years 1996 and 1997 in Mace Head. The solid line shows REMO simulation at the lowest model layer, except at SCH (730 m asl in July and 1200 m otherwise) and at JFJ (2850 m asl). TM3 results are represented by the thin solid line.

station (Schmidt et al., 1996). At **Jungfraujoch** both TM3 and REMO sampled at layer 5 (2850 m) reproduce correctly the measured RA, with REMO showing a more realistic phase than TM3. In September REMO and TM3 reach their maximum earlier in the day than observed. This is most probably due to their inability to account for vertical mixing induced by the local topography.

6.3. Seasonal cycle

At **Mace Head** the low monthly mean ^{222}Rn value in March 1998 is well reproduced in REMO and TM3 (Fig. 11) and both models correctly simulate the mean for other months. At **Zingst** monthly values are generally a factor of two higher than the observation, and consequently, the simulated variability within each month is also overestimated. The seasonal cycle amplitude, however, is in correct agreement with the data, with a decrease from April to August and a rise in September. At **Heidelberg** REMO and TM3 match the data well, without any well defined annual cycle. The variability in the models is too small in August, September and May. At **Schauinsland** the data show a seasonal cycle, with a maximum in August and a minimum in March. REMO sampled at 1200 m (layer 4) matches the data well in spring and in autumn, whereas the 730 m (layer 1) layer matches the summer data best. Neither REMO nor TM3 is nonetheless able to reproduce the maxima in August and in September. At **Jungfraujoch** a seasonal cycle is apparent in the data (Lugauer, 2000) with maximum values in May, associated with the largest variability, and minimum values in October. Both TM3 and REMO models reproduce the monthly data within 0.5 Bq m^{-3} when sampled at the actual altitude of JFJ, except in April and May. Both models, however, do not produce a realistic seasonal cycle, and underestimate the variability. On the other hand, when sampled closer to the surface, the models generate a monthly variability that is comparable with the data, but in that latter case, it grossly overestimates the mean values.

7. Site effects and data selection in models using ^{222}Rn

Radon-222 is influenced by "site effects" specific to continental stations, such as the impact of local sources and local topography, which are difficult to capture at the current resolution of models.

Mountain stations records are difficult to represent even in a relatively high-resolution model (e.g. SCH). Attention must be given to locate the station at an adequate altitude in the vertical discretisation of the model, knowing that local topography is not resolved by the models. Vertical gradients (Freiburg–Schauinsland difference) data provide here a key validation of the intensity of vertical mixing. At mountain stations such as SCH, we learned from ^{222}Rn that the observed and modelled air temperatures can be used to pick up the "best" altitude to sample the model output. To be able to reproduce in the simulated temperature a diurnal cycle as observed, one should pick up the first model box near the surface at the end of March, in July and at the beginning of October. On the other hand, for matching small diurnal cycles in the temperature indicating free tropospheric air, one should rather pick up the model layer at the actual altitude of the station. Locating a mountain station at varying altitudes in the model using these simple criteria based on daily temperature changes greatly improves the agreement between measurements and models. Such criteria could be generalised to the selection of other tracers such as CO_2.

Coastal stations close to large continental areas are also difficult to model (e.g., ZGT). The main problem is to select the model grid cell that best corresponds to the station. In our case, ZGT is located in a land grid cell which emits ^{222}Rn, and therefore the simulated values are likely overestimated. This problem has also been recognised in global studies dealing with CO_2 (Ramonet et al., 1996) and is commonly addressed by sampling the model output at coastal sites in the next upwind grid cell in the sea. In REMO, the northern, eastern and western grid cells next to ZGT are in the Baltic Sea, whereas the next southern grid cell is on land. We accordingly selected the model output on nearby grid cells depending on the direction of the wind. For instance, if the wind comes from the north, the ZGT grid cell is moved in REMO to the next grid cell north. Thanks to this data selection, the simulated concentration (Fig. 12b) comes into a better agreement with the observations when the wind is coming from the sea. However, when the wind is from the land, the modelled ^{222}Rn concentration is still too high compared to the data, which probably reflects an overestimation of ^{222}Rn emissions over the Baltic plains (Schmidt, 1999). Using high-resolution models to transport CO_2 implies a careful selection of model output at coastal stations. Usually, in global studies for CO_2 (e.g., Bousquet et al., 1999; Gurney et al., 2002) coastal stations are simply shifted one box into the sea. This simple recipe would not hold within a high-resolution model such as REMO, where the land–sea contrast in CO_2 concentration will be much sharper than in a coarse grid model. We rather suggest that, based on the ^{222}Rn simulation at ZGT and also at MHD, the data selection in models at coastal sites can be carried out using wind direction and wind speed criteria. An even better method if both ^{222}Rn and CO_2 measurements are available would be to select the CO_2

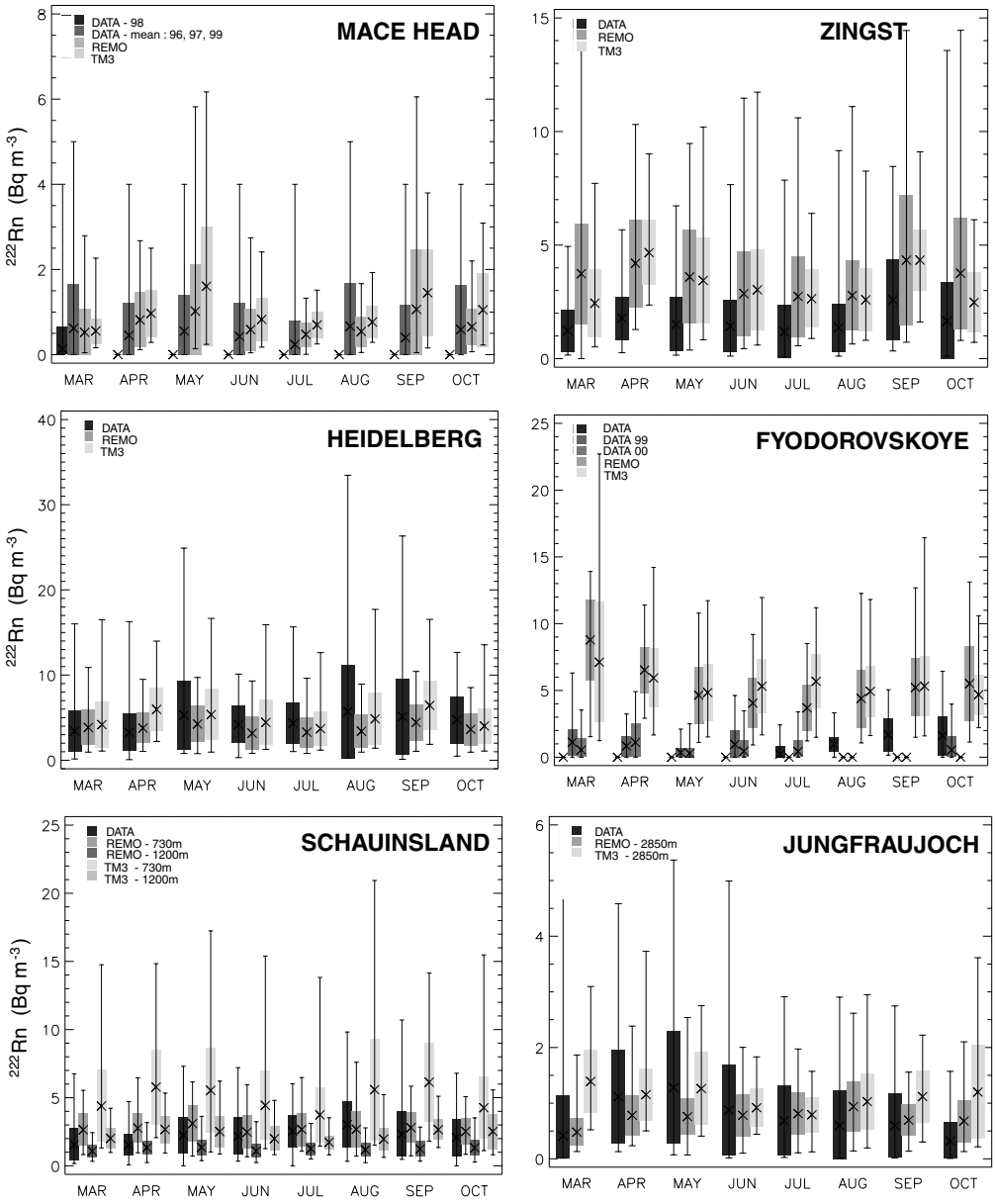

Fig. 11. Seasonal cycle of ^{222}Rn concentration at six stations in Europe. Measurements are in dark grey; REMO simulations are represented by darker grey when going higher in altitude. TM3 results are represented by the lightest grey. The inbox cross indicates the monthly mean value of ^{222}Rn concentration. Extremities of the vertical box show the 1σ standard deviation, and extremities of the vertical line present the minimum and maximum of the concentration.

simulation only when simulations best match the ^{222}Rn records, as first suggested by Ramonet et al. (1996).

Site effects for ^{222}Rn also encompass uncertainties in local to regional emissions near a station, which often imply that the model does a poor job at reproducing the observations. Two such examples are the discrepancy between REMO and data at TVR and at ZGT. Both stations are located in plains where, during

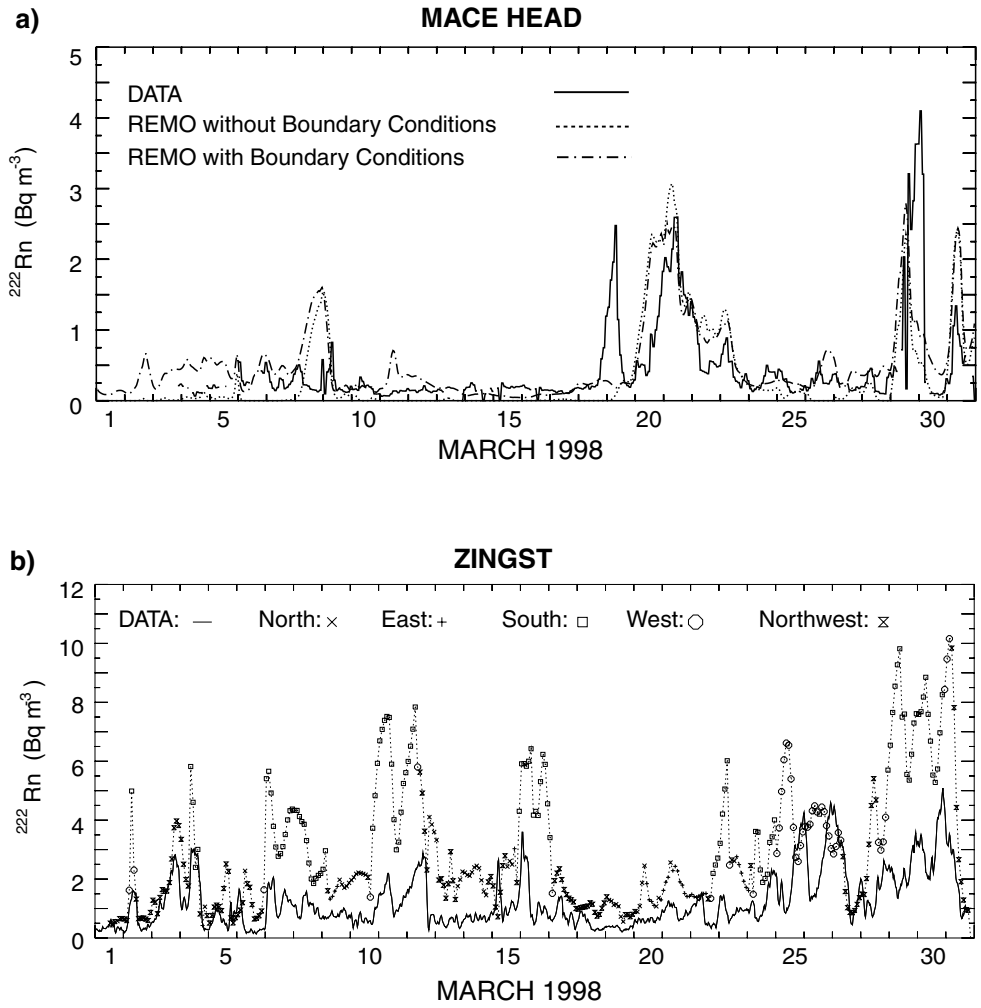

Fig. 12. (a) Impact of ^{222}Rn prescribed as REMO boundary conditions on simulation at Mace Head during March 1998. Measurements are presented by the solid line, the ^{222}Rn simulation with zero boundary conditions by the dashed line and the standard simulation by the dash-dot line. (b) ^{222}Rn concentration resulting from the "box shifting" method in Zingst during March 1998. Measurements are solid line; shown by a symbols denote simulated concentrations in the northern (×), eastern (+), southern (square), western (circle) and north-western (double triangle).

rainy periods, water saturating the soils blocked the exhalation of ^{222}Rn to the atmosphere. As a sensitivity test to study the influence of the ^{222}Rn source, we replaced uniform emissions by a soil type dependent emission map, based on soil types (Food and Agriculture Organisation, UNESCO, Paris, 1970–1978) and ^{222}Rn emissions measured by Eckhardt (1990). In that map, emissions range from 0.3 atom cm^{-2} s^{-1} in peat up to 1.5 atom cm^{-2} s^{-1} in clay, but the rate of emission is constant with time. The differences in ^{222}Rn concentration between this sensitivity experiment and our standard run (1 atom cm^{-2} s^{-1}) consist mainly of distinct large scale spatial patterns. None of those differences could bring REMO at TVR and ZGT into a better agreement with observations. This suggests that the soil moisture content, beyond the soil type, is a major variable in controlling ^{222}Rn emissions. To test the impact of local source further, all ^{222}Rn sources near TVR (150 km × 150 km) were switched off. In July this was sufficient to match the data, whereas in

October the data were still overestimated, probably indicating that low emissions from soils over a large area around the station are affecting the measurement point.

The resolution of REMO is finer than the one of most global models that were used for ^{222}Rn simulations, yielding to a better capture of the synoptic variability than in TM3. In addition, the meteorological forcing, which is processed only at the lateral boundaries of REMO domain, only determines the large-scale flow pattern, whereas the model is free to compute its own climate inside the domain. This may locally cause large differences in the flow fields, compared to observations, and consequently in the transport of the tracers. Thus the model TM3, which uses ECMWF analysis in the full domain, may simulate more realistic concentrations than REMO, despite its coarser resolution (e.g. ZGT). Chevillard et al. (2002) have shown that, over Europe, REMO simulates a more realistic climate when it is run in a "forecast mode", with ECMWF boundary and initial conditions being restored each 30 h, than in the "climate mode" used in this work. However, we observed that the ^{222}Rn concentrations simulated with the "forecast version" of REMO do not strongly improve as compared to the "climate mode" results, which implies that uncertainties in the ^{222}Rn simulations are mainly due to the uncertain ^{222}Rn source or to local-scale transport not resolved in the actual horizontal resolution.

8. Conclusions

We performed a simulation of ^{222}Rn using the regional model REMO, and compared the results with the one of the global coarser model TM3 and with observations in Europe. Comparing the two models with the data makes it possible to determine which one performs best, in order to analyse whether a significant improvement occurs when using a higher-resolution tracer code. The large number of ^{222}Rn measurement sites in Europe, and the fact that all those records are continuous, provides a unique test bed for transport models, going from diurnal and synoptic to seasonal time scales. We analysed "site effects" at mountain and coastal stations, and formulated some model output selection criteria to obtain more realistic simulations, which have implications for CO_2 model–data comparison as well.

Overall, both REMO and TM3 perform rather well to reproduce the ^{222}Rn synoptic variability, mostly linked to meteorology. They also both capture diurnal changes in ^{222}Rn at inland stations, which reflect the modulation of surface emissions by the oscillation of the boundary layer height. We noticed, however, that ^{222}Rn emissions are certainly not uniform in space (and in time as well) across Europe, and not accounting for this in models leads to a mismatch with the observed mean values and diurnal cycle amplitudes. Using the relative amplitude to evaluate model–data agreement enabled us to overcome this problem. From our results, we can not say that REMO is better than TM3 or vice-versa. Improvements in REMO as compared to TM3 are visible at short time scales, with REMO better reproducing synoptic "events" and daily variations. REMO is more realistic at SCH (mountain), when the appropriate model vertical layer is selected. TM3 is more realistic at ZGT (coast), where the coarse resolution may compensate for contrasted land/ocean emissions. Finally, both models equally succeed at HDG and fail at TVR to reproduce repeated diurnal cycles of ^{222}Rn, pointing to the fact that the current (systematic) uncertainty on ^{222}Rn emissions from soils is more important than differences among transport models in terms of matching models with observations.

9. Acknowledgements

We thank our partners from the EUROSIBERIAN CARBONFLUX EU project and especially all the field workers at the observational sites. The work was partly funded by the European Commission under contract no. ENV4-CT97-0491 (EUROSIBERIAN CARBONFLUX). We thank the ECMWF for providing surface and model level analysis data. We also acknowledge the support of C. Boonne (IPSL's Pole données) for extracting the data.

REFERENCES

Biraud, S., Ciais, P., Ramonet, M., Simmonds, P., Kazan, V., Monfray, P., O'Doherty, S., Spain, G. T. and Jennings, G. S. 2000. European greenhouse gas emissions estimated from continuous atmospheric measurements and radon-222 at Mace Head, Ireland. *J. Geophys. Res.* **105**, 1351–1366.

Bousquet, P., Gaudry, A., Ciais, P., Kazan, V., Monfray, P., Simmonds, P. G. and Jennings, G. S. 1996. Atmospheric

CO_2 concentration variations recorded at Mace Head, Ireland, from 1992 to 1994. *Phys. Chem. Earth* **21**, 477–481.

Bousquet, P., Peylin, P., Ciais, P., Ramonet, M. and Monfray, P. 1999. Optimisation of annual atmospheric CO_2 net sources and sinks using inverse modeling. Part 2: sensitivity study. *J. Geophys. Res.* **104**, 26179–26193.

Chevillard, A., Karstens, U., Ciais, P., Lafont, S. and Heimann, M. 2002. Simulation of atmospheric CO_2 over Europe and western Siberia using the regional scale model REMO. *Tellus* **54B**, this issue.

Cuntz, M. 1997. The Heidelberg ^{222}radon monitor: Calibration, optimisation, application. Thesis, Institut für Umweltphysik, University of Heidelberg (in German).

Dentener, F., Feichter, J. and Jeuken, A. 1999. Simulation of the transport of ^{222}Rn using on-line and off-line models at different horizontal resolutions: a detailed comparison with measurement. *Tellus* **51B**, 573–602.

Dörr, H. and Münnich, K. O. 1990. ^{222}Rn flux and soil air concentration profiles in West Germany. Soil Rn as tracer for gas transport in the unsaturated soil zone. *Tellus* **42B**, 20–28.

Eckhardt, K. 1990. Measurement of radon flux and of its dependence with soil conditions. Thesis, Institut für Umweltphysik, University of Heidelberg (in German).

Gäggeler, H. W., Jost, D. T., Baltensperger, U., Schwikowski, M. 1995. Radon and thoron decay product and 210Pb measurements at Jungfraujoch, Switzerland. *Atmos. Environ.* **29**, 607–616.

George, A. C. 1981. Radon flux measurement. In: *USDOE rpt. EML-399* Environmental Measuring Laboratory, U.S. Dept. of Energy, New York, 207–212.

Gurney, K. R., Law, R. M., Denning, S. A., Rayner, P. J., Baker, D. et al., 2002. Towards robust regional estimates of CO_2 sources and sinks using atmospheric transport models. *Nature* **415**, 626–630.

Heimann, M. 1995. The global atmospheric tracer model TM2. *Technical report no.10*, Deutsches Klimarechnenzentrum (DKRZ), Hamburg, Germany.

Heimann, M., Monfray, P. and Polian, G. 1990. Modeling the long range transport of ^{222}Rn to Subantarctic and Antarctic areas. *Tellus* **42B**, 83–99.

Jacob, D. and Potzun, R. 1997. Sensitivity studies with the regional climate model REMO. *Meteor. Atmos. Phys.* **63**, 119–129.

Jacob, D. J. and Prather, M. J. 1990. Radon-222 as a test of convective transport in a general circulation model *Tellus* **42B**, 118–134.

Jacob, D. J., Prather, M. J., Rasch, P. J., Shia, R.-L., Balkansky, Y. J. et al., 1997. Evaluation an intercomparison of global atmospheric transport models using ^{222}Rn and other short-lived tracers. *J. Geophys. Res.* **102**, 5953–5970.

Karstens, U., Nolte-Holube, R. and Rockel, B. 1996. Calculation of the water budget over the Baltic catchment area using the regional forecast model REMO for June 1993. *Tellus* **48A**, 684–692.

Lambert, G., Polian, G., Sanak, J., Ardouin, B., Buisson, A., Jegou, A. and Leroulley, J. C. 1982. ^{222}Rn cycle and its daughters: applications to the troposphere–stratosphere exchange study. *Ann. Géophys.* **38**, 497–531.

Langmann, B. 2000. Numerical modeling of regional scale transport and photochemistry directly together with meteorological processes. *Atmos. Environ.* **34**, 3585–3598.

Levin, I., Graul, R. and Trivett, N. B. A. 1995. Long-term observations of atmospheric CO_2 and carbon isotopes at continental sites in Germany. *Tellus* **47B**, 23–34.

Levin, I., Born, M., Cuntz, M., Langendörfer, U., Mantsch, S., Naegler, T., Schmidt, M., Varlagin, A., Verclas, S. and Wagenbach, D. 2002. Observations of atmospheric variability and soil exhalation rate of radon-222 at a Russian forest site: Technical approach and deployment for boundary layer studies. *Tellus* **54B**, this issue.

Liu, S. C., McAfee, J. R. and Cicerone, R. J. 1984. Radon-222 and tropospheric vertical transport. *J. Geophys. Res.* **89**, 7291–7297.

Louis, J.-F. 1979. A parametric model of vertical eddy fluxes in the atmosphere. *Boundary Layer Meterol.* **17**, 187–202.

Lugauer, M., Baltensperger, U., Furger, M., Gäggeler, H. W., Jost, D. T., Schwikowski, M. and Wanner, H. 1998. Aerosol transport to the high alpine sites Jungfraujoch (3454 m asl) and Colle Gnifetti (4452 m asl). *Tellus* **50B**, 76–92.

Lugauer, M., Baltensperger, U., Furger, M., Gaggeler, H. W., Jost, D. T., Nyeki, S. and Schwikowski, M. 2000. Influences of vertical transport and scavenging on aerosol particle surface area and radon decay product concentrations at the Jungfraujoch (3454 m above sea level). *J. Geophys. Res.* **105**, 19869–19879.

Majewski, D. 1991. The Europa model of the Deutscher Wetterdienst. *Semin. Proc. ECMWF* **2**, 147–191.

Mellor, B. and Yamada, T. 1974. A hierarchy of turbulence closure models for planetary boundary layers. *J. Atmos. Sci.* **31**, 1791–1806.

Nazaroff, W. N. 1992. Radon transport from soil to air. *Rev. Geophys.* **30**, 137–160.

Nyeki, S., Baltensperger, U., Colbeck, I., Jost, D. T., Weingartner, E. and Gäggler, H. W. 1998. The Jungfraujoch high-alpine research station (3454 m) as a background clean continental site for the measurement of aerosol parameters. *J. Geophys. Res.* **103**, 6097–6107.

Ramonet, M. 1994. Variabilité du CO_2 atmosphérique en régions australes: Comparaison modèle-mesures. Ph.D. Thesis, Université de Paris 6, France.

Ramonet, M., Le Roulley, J. C., Bousquet, P. and Monfray, P. 1996. Radon-222 measurements during TROPOZ II compaign and comparison with a global atmospheric transport model. *J. Atmos. Chem.* **23**, 107–136.

Russel, G. and Lerner, J. 1981. A new finite-differencing scheme for tracer transport equation. *J. Appl. Meteorol.* **20**, 1483–1498.

Schmidt, M. 1999. Measurement and balancing anthropogenic greenhouse gases in Germany. Ph.D. Thesis, University of Heidelberg, Germany.

Schmidt, M., Graul, R., Sartorius, H. and Levin, I. 1996. Carbon dioxide and methane in continental Europe: a climatology, and 222-radon-based emission estimates. *Tellus* **48B**, 457–473.

Smolarkiewicz, P. K. 1983. A simple positive definite advection scheme with small implicit diffusion. *Mon. Weather Rev.* **111**, 479–486.

Tiedtke, M. 1989. A comprehensive mass flux scheme for cumulus parameterization in large scale models. *Mon. Weather Rev.* **117**, 1779–1800.

Turekian, K. K., Nozaki, Y., Benninger, L. K. 1977. Geochemistry of atmospheric ^{222}Rn and ^{222}Rn products. *Ann. Rev. Earth Planet. Sci.* **5**, 227–255.

Whittlestone, S., Zahorowski, W. and Schery, S. D. 1998. Radon flux variability with season and location in Tasmania, Australia. *J. Radioanal. Nucl. Chem.* **236**, 1–2, 213–217.

Wilkening, M. H. and Clements, W. E. 1975. Radon-222 from the ocean surface. *J. Geophys. Res.* **80**, 3828–3830.